Hydrol. Earth Syst. Sci. Discuss., 9, 6935–6977, 2012
www.hydrol-earth-syst-sci-discuss.net/9/6935/2012/
doi:10.5194/hessd-9-6935-2012

Hydrology and Earth System Sciences Discussions

High resolution reconstruction of monthly precipitation of Iberian Peninsula using circulation weather types

N. Cortesi[1,2], R. Trigo[2], J. C. Gonzalez-Hidalgo[1,3], and A. M. Ramos[4]

[1]University of Zaragoza, Department of Geography, Spain
[2]University of Lisbon, CGUL, IDL, Lisbon, Portugal
[3]Instituto Universitario Ciencias Ambientales (IUCA), University of Zaragoza, Spain
[4]University of Vigo, Ephyslab, Vigo, Spain

Received: 30 March 2012 – Accepted: 17 May 2012 – Published: 4 June 2012

Correspondence to: J. C. Gonzalez-Hidalgo (jcgh@unizar.es)

Published by Copernicus Publications on behalf of the European Geosciences Union.

Abstract

Precipitation over the Iberian Peninsula (IP) is highly variable and shows large spatial contrasts between wet mountainous regions, to the north, and dry regions in the inland plains and southern areas. In this work, a high-density monthly precipitation dataset for the IP was coupled with a set of 26 atmospheric circulation weather types (Trigo and DaCamara, 2000) to reconstruct Iberian monthly precipitation from October to May with a very high resolution of 3030 precipitation series (overall mean density one station each 200 km^2). A stepwise linear regression model with forward selection was used to develop monthly reconstructed precipitation series calibrated and validated over 1948–2003 period. Validation was conducted by means of a leave-one-out cross-validation over the calibration period. The results show a good model performance for selected months, with a mean coefficient of variation (CV) around 0.6 for validation period, being particularly robust over the western and central sectors of IP, while the predicted values in the Mediterranean and northern coastal areas are less acute. We show for three long stations (Lisbon, Madrid and Valencia) the comparison between model and original data as an example to how these models can be used in order to obtain monthly precipitation fields since the 1850s over most of IP for this very high density network.

1 Introduction

Understanding precipitation variability is crucial to assess recent significant climate trends and predictions, to calibrate regional models, to quantify changes in the hydrological cycle and to develop national and regional water planning. However, precipitation variability is difficult to assess because precipitation is one of the climate elements with highest variability at temporal and spatial scale. This explains the generalized recommendation of high density precipitation which requires a database for regional analyses.

HESSD
9, 6935–6977, 2012

In Europe one of the most important areas to study precipitation variability is the Iberian Peninsula (IP) because of its latitudinal location (between tropical and mid latitudes), its western position contrasting between two water bodies (Atlantic ocean and Mediterranean Sea), and also because the disposition of the main relief chain in central and western areas is West-East, while to the East the relief is North-South. Thus precipitation in the IP exhibits high variability at spatial and temporal domains (de Castro et al., 2005; de Luis et al., 2008).

In the IP precipitation presents the largest concentration from October to May, mainly due to the baroclinic synoptic-scale perturbations moving eastward from the Atlantic Ocean, although mesoscale convective systems are also responsible for high rainfall rates in the eastern half of the Iberian Peninsula (Paredes et al., 2006; García-Herrera et al., 2005). In contrast, the scarce summer precipitation is mostly due to local factors and convective storms (Serrano et al., 1999). Furthermore, seasonal precipitation regimes in the IP exhibit a great variability, and dramatic changes during the second half of the 20th century have been detected mostly by the effect of spring precipitation decrease (de Luis et al., 2010). For these reasons, rainfall spatial variability in the IP can be detected only using a spatially dense network of observations (Auer et al., 2005; Brunetti et al., 2006; Valero et al., 2009; Gonzalez-Hidalgo et al., 2009).

In recent years, significant efforts were made to reproduce precipitation behaviour in Europe with a particular focus in the IP from daily to seasonal scales, using an array of methods including circulation weather types (WTs). The usefulness of WTs classification has been investigated for a wide range of applications in scientific domains, from climate to environmental areas such as air quality, and increasingly for natural hazards such as forest fires, floods, droughts, avalanches and storm lightning (e.g. Demuzere et al., 2009; Prudhomme and Genevier, 2011; Kassomenos, 2010; Ramos et al., 2011). From an hydrological perspective, WTs classifications have been used for different purposes, including their relation with precipitation (e.g. Hanggi et al., 2011; Andrade et al., 2011), drought (e.g. Fowler and Kilsby, 2002; Fleig et al., 2011) and river discharge, including floods (e.g. Wilby, 1993; Auffray et al., 2011; Fowler et al., 2000).

HESSD
9, 6935–6977, 2012

The main objective of all circulation classification schemes is to provide fast, objective and reproducible methods for categorizing the continuum of atmospheric circulation into a reasonable and manageable number of discrete classes (types). Different methods exist for the classification of circulation weather types (WTs), as was shown by Huth et al. (2008), and Phillip et al. (2010). These different methodological approaches can be categorized by the kind of type definition they use that can range from pure statistical (e.g. Cluster analysis and PCA) or dynamic based (e.g. intensity and direction of geostrophic wind and vorticity).

Regarding the use of WTs classification for downscaling, Bárdossy and Pegram (2011) define procedures to give confidence in the interpretation of such rainfall estimates modelled by global circulation models (GCMs). They use circulation patterns to define quantile-quantile transforms between observed and GCMs estimated rainfall in present climate and to estimate the rainfall patterns in future scenarios. Wilby (1998), modeled low-frequency rainfall events by means of: airflow indices, WTs classifications and frontal frequencies. Distinct circulation weather type clusters were identified and used to construct a simplified model of daily precipitation amount. The model was calibrated against station data for the period 1970–1990 and used to reconstruct observed daily precipitation between 1875 and 1969 given the historic sequence of WTs.

In the Iberian Peninsula, Goodess and Palutikof (1998) developed a Markov Chain model to reconstruct daily precipitation at 20 locations in Guadalentin Basin (SE Spain) using 8 WTs as predictor variables. Trigo and DaCamara (2000) introduced a multiple regression model based on the three wettest WTs frequencies (the cyclonic, the south westerly and the westerly types) as predictor variables to reconstruct monthly winter rainfall totals for 18 key sites in Portugal. Spellman (2000) performed a stepwise regression analysis on a catalogue of air flow indexes to estimate monthly mean rainfall amounts for IP. Goodess and Jones (2002) expanded the regression model to include up to 14 circulation weather-types frequencies with a forward selection method based on the F-test and applied to 20 Iberian stations. Finally, Santos et al. (2005) developed a K-mean cluster analysis over the first three principal components of the daily

HESSD
9, 6935–6977, 2012

sea-level pressure weighted anomalies to isolate 5 weather regimes responsible for the inter annual variability of monthly winter rainfall amounts.

However, all the above mentioned works addressing the link between monthly winter precipitation and atmospheric circulation patterns relied on low density observation networks to calibrate their models (typically less than 50 stations for the whole IP). In this regard it is perfectly reasonable to state that the spatial detail required for hydrological planning, soil erosion, and many other purposes were not well captured. Also spring, summer and autumn precipitation variability were less explored, notwithstanding October–April are the most rainiest period in many areas in the IP (de Luis et al., 2010). In these sense, the recent developing of high density spatial database of monthly precipitation in the IP combining Portugal and Spanish land (see Gonzalez-Hidalgo et al., 2011; Lorenzo et al., 2011) provide for the first time an opportunity to fill this gap and facilitates the relationships between weather types and precipitation totals at high spatial detail.

Accordingly, the objective of this paper is the development of a model based on WTs to calibrate and validate monthly precipitation totals in the IP. The research is conducted not on precipitation variability itself, but on the nature of its variability. This paper is the starting step to provide the opportunity of extending the reconstruction of monthly precipitation at very high resolution as far back in time as 1850, because catalogues of circulation weather types are now available since then. These reconstructions at high spatial detail would provide in the near future the long-term contextual framework of precipitation variability and trends in the IP, thus allowing considering the recent changes of precipitation monthly distribution within a more global context from the middle of the 19th century. Therefore, while the main effort of this paper is centred on the evaluation of models performance during the 1948–2003 calibration/validation period, we will also assess the potential of this modelling approach by applying the validation with three of the longest series of monthly precipitation available in the IP.

The model selected was a forward stepwise linear regression derived from that of Trigo and DaCamara (2000) and of Goodess and Jones (2002). It uses 26 WTs as predictor variables, and monthly rainfall totals as the predicted variable. Like many other rainfall models, the validation method was developed only for the October to May months, because most IP precipitation falls within these months (roughly 80 %). Moreover, changes in summer rainfall cannot always be explained by changes in circulation, given that local factors play a major role (Mosmann et al., 2004). Finally, monthly reconstruction was preferred, because seasonal trend analysis often masks different monthly trends in the IP precipitation (Serrano et al., 1999; Goodess and Jones, 2002; Gonzalez-Hidalgo et al., 2009; de Luis et al., 2009).

The paper is organized as follows. Section 2 describes the data, circulation weather types used, description of the model and the validation method. Section 3 analyses the model performance and the relative contribute to total monthly precipitation of each WT. The following two sections are devoted to two useful hydrological applications of this methodology namely to reconstruct long-term precipitation (Sect. 4) and to reproduce long-term river flow variability of three large Iberian rivers (Sect. 5). Finally, Sect. 6 contains a summary of the main results and the concluding remarks.

2 Database, weather types and methods

2.1 Precipitation data

We used a dense network of monthly precipitation series from MOPREDAS database (MOnthly PREcipitation DAtabase of Spain) for Spanish land (Gonzalez-Hidalgo et al., 2011) and a Portuguese database from INAG – Instituto da Água (Servicio Nacional de Informaçao de Recurcos Hídricos) (Lorenzo et al., 2011). In this research, the total amount of series are 2644 and 386 for Spain and Portugal respectively conterminous land, and the spatial distribution is presented in Fig. 1. The series come from an exhaustive quality control of original information, and the series are free of anomalous data and inhomogeneities (details can be found in Gonzalez-Hidalgo et al., 2011; Lorenzo et al., 2011). At present the dataset is the most complete and extensive

HESSD
9, 6935–6977, 2012

monthly precipitation database available in IP, and it allows to combine a high station density with a long reconstruction period. In this research, the selected period was 1948–2003 with an overall spatial density of 1 observatory/200 km^2. In general terms, the spatial distribution is quite homogeneous all over the IP, being lower in Galicia (NW IP), Extremadura (W) and Pyrenees (NE). In any case it should be stressed that this is the work with the highest density of stations covering the entire IP. Additionally we have used precipitation values for three very long monthly precipitation series of IP (Lisbon, Madrid and Valencia) with common data between 1864 and 2003.

2.2 Circulation data and weather type classification

This study relies on a daily historical European-North Atlantic mean sea level pressure dataset produced for 1850–2003 on a 5° latitude by longitude grid and compiled by Ansell et al. (2006) in the framework of the EMULATE project. The daily circulation weather types affecting IP are characterized through the use of a set of indices adopted by Trigo and DaCamara (2000) who take into account physical or geometrical considerations, such as the direction and strength of airflow, direction and vorticity of geostrophic flow, and degree of cyclonicity. This classification is based on the corresponding objective classification defined for the British Isles (Jenkinson and Collison, 1977; Jones et al., 1993) and has been broadly used for studying climate variability in the region like: trends of Iberian precipitation (Spellman, 2000; Goodess and Jones, 2002; Paredes et al., 2006), extreme events assessment such as droughts (Garcia-Herrera et al., 2007), wet winters (Vicente-Serrano et al., 2011) or even relationship with modes of low frequency variability (Ramos et al., 2010). Furthermore, this methodology has also been also used for the construction of climate change scenarios (Goodess and Palutikof, 1998; Miranda et al., 2002) and even linking storm lightning activity to atmospheric circulation (Tomás et al., 2004; Ramos et al., 2011). The set of indices was computed using sea level pressure (SLP) values obtained for the 16 grid points and shifted 5° to the east compared with the original study of Trigo and DaCamara (2000), in order to centre the study area (Iberia Peninsula) in the grid flow indices (Fig. 2).

The indices mentioned allow us to define 26 different circulation Weather Types (WTs) at daily level and for the study period; 8 WTs are purely directional types (NE, E, SE, S, SW, W, NW and N, see Fig. 3); 2 WTs are dominated by the strength of vorticity (cyclonic C and anticyclonic A types); and 16 other WTs are hybrid types (8 for each C or A hybrid, see Table 1). The conditions established to define the different circulation weather types are the same as in Trigo and DaCamara (2000). Unlike some other authors (Jenkinson and Collison, 1977; Jones et al., 1993), an unclassified class was not defined, opting to disseminate the fairly few cases (<2 %) with possibly unclassified situations among the retained classes. For model performance usually WTs classifications using a smaller number of WTs are recommended, because in this case each predictor WT benefits of a higher number of days for month, and then regression analyses is improved. We tried this approach with 10 WTs, and the resulting model performance, measured with the global Coefficient of Variation (CV) score (see Sect. 2.3.1), was 0.60; for 18 WTs it was found to be 0.57; and finally the CV with 26 WTs was 0.55. This means that 26 WTs improved the regression performance up to 8 % compared to what was achieved using 10 WTs only, so the classification with 26 WTs was selected for all the following analysis.

2.3 River flow data

Monthly river flow data were provided by the Portuguese Institute of Water (INAG) for river Guadiana, Tagus and Douro and is restricted to the period 1956–2006, that has been used in previous applications by some of us (Trigo et al., 2004; Gámis-Fortis et al., 2010) and has been intensively checked for inconsistencies. The location of the river gauges within the Portuguese section of the rivers is depicted in Fig. 1, and the main characteristics of the flow measured at these gauges can be seen in Table 2.

HESSD
9, 6935–6977, 2012

2.4 The model

In order to develop a monthly precipitation reconstruction of Iberian rainfall, a stepwise linear regression analysis (forward selection) was performed from 1948 to 2003. The model was applied individually to all 3030 Iberian precipitation series and for the eight separate months (from October to May). The 26 daily WTs were grouped into monthly mean values and used as potential predictor variables and monthly rainfall totals as predicted variable. Regression analysis was performed only for autumn, winter and spring months (strictly speaking from October to May), because correlations between WTs and rainfall amounts are much stronger than during summer months and because absolute amounts of precipitation due to convective processes is relatively lower during the selected months.

We select the forward selection criteria to minimize the over fitting of WTs in the regression, to separate noise from the dominant temporal patterns of variability, and to remove correlated predictor variables from the subset of predictors chosen for a given series and month. Thus, the selection processes of WTs are crucial for the reconstruction, because the model performance largely depends on the input variables (von Storch and Zwiers, 1999).

In this work, the criterion to select WTs at each step was as follows: at each step k in the process, we checked if each new potential predictor (WTs) contribution decreased the Coefficient of Variation (CV). We followed this criterion because it is the most commonly used in cases where there is a large number of explanatory variables and no underlying theory on which to base the predictor's selection (Wilks, 2005; Efroymson, 1960). Moreover the CV is unitless allowing values obtained for different stations to be compared to each other in ways that other measures, such as the root mean squared residuals or the standard deviations cannot be. Thus we checked all the potential predictors in all the steps of the model.

The CV is defined as the ratio between the Root Mean Square Error (Eq. 1) and the observed mean monthly precipitation $\bar{O}$, for the selected series s, month m and regression step k as follows:

Discussion Paper | Discussion Paper | Discussion Paper | Discussion Paper |

HESSD

9, 6935–6977, 2012

High resolution reconstruction of monthly precipitation

N. Cortesi et al.

Title Page
Abstract Introduction
Conclusions References
Tables Figures
Back Close
Full Screen / Esc
Printer-friendly Version
Interactive Discussion

$$\mathrm{RMSE}(s,m,k) = \sqrt{\frac{\sum_{i=1}^{n}(P_i(s,m,k) - O_i(s,m))^2}{n}} \quad (1)$$

And the CV (2):

$$\mathrm{CV}(s,m,k) = \frac{\mathrm{RMSE}\ (s,m,k)}{\bar{O}(s,m)} \quad (2)$$

with ***P*** and ***O*** being two vectors with respectively the predicted and observed monthly precipitation values for all the $n = 56$ yr of the regression period (1948–2003). The CV is a non negative number that tends to 0 when there is perfect agreement between reconstructions and observations.

The procedure was finished when, for all the new variables introduced in a given step k, the CV did not decrease of at least 0.01 in comparison to the CV of the previous step $k-1$. This threshold was equivalent to improve the root mean square error of 10 mm of precipitation in a mean monthly observed precipitation of 1000 mm. The proposed threshold value was also chosen because at the same time it minimised the numbers of predictors without significantly decreasing the model performance measured by the CV scores.

For each step k, the regression coefficients were calculated solving a non-negative least-squares problem because each coefficient physically represents the mean rainfall amount of the correspondent WT that is non-negative by definition. The constant term was also constrained as non-negative, because it can be interpreted as the rain amount due to processes which can not be modelled solely by WTs, but whose rain amount for a given month should be constant from one year to the next (i.e: convective processes). Up to a maximum of eight predictors were selected for individual series.

It is important to stress that each regression coefficient represents the mean predicted total rainfall amount due to its associated WT. Therefore, multiplying each coefficient for the mean number of days belonging to the same WT returns the mean

HESSD
9, 6935–6977, 2012

predicted monthly precipitation due to the chosen WT during period 1948–2003. To compare series with different total rainfall amounts it is more convenient to analyze the relative estimated contribution of each WT to mean monthly predicted precipitation, dividing the absolute estimated contribution of each WT by the total monthly precipitation for the mean observed monthly precipitation in the same period.

At the end of the selection of the best predictor WTs, a small number of them (0.3 %) were still moderately correlated ($r \approx 0.4$–0.5). Usually, to overcome multicollinearity problems, "... *whichever of the two high correlated WTs is picked at a later regression step is omitted from the final set of predictor variables*" (Goodess and Jones, 2002). However, we did not remove any correlated WTs because correlations were not high and because multicollinearity does not reduce the predictive power or the model, i.e.: it only affects calculations regarding the independent variables and their coefficients.

Model validation was performed by means of a leave-one-out cross-validation (also known as "Jack-knife") over the regression period for all 3030 series of monthly precipitation of IP. We applied this validation method because it is independent from any subset of years that might be chosen as a representative subset random sample. In the Jack-knife procedure, a single monthly observation from the original sample is used as the validation data, and the remaining observations as the training data. Specifically, for the period 1948–2003, each monthly year data was sequentially removed and the remainder (56 yr) used to calibrate the regression model for that month that was then used to predict the rainfall for the omitted year.

We used two estimators to measure the model validation: the coefficient of variation CV (defined by Eqs. 1 and 2), and the Pearson's Product moment correlation coefficient r, between the observed and the reconstructed precipitation.

HESSD
9, 6935–6977, 2012

3 Results

3.1 Model validation

The results of the cross-validation analysis are shown in the following set of Figs. 4 and 5 that focus on different aspects of the evaluation procedure. The area where we found the highest values of r Pearson are located to the North-West (North of Portugal and Spanish border) during December ($r > 0.9$) (Fig. 4). Also high values of r between 0.7 and 0.9 are located to the West and South-West except in April and May when high values are restricted to the Northern areas of Portugal, and surrounding areas of Spain. The lowest values are found in the Mediterranean fringe but the area with $r < 0.5$ varies between months. It is interesting to notice that the Ebro basin to the northeast inland of IP usually exhibits moderate values ranging between 0.5–0.7. In general the spatial diversity of r-values increases in April and May suggesting that precipitation depends more on local factors during these months.

The obtained spatial pattern of parameter r suggests that the capacity of using regional atmospheric circulation classes to explain the Iberian precipitation regime decreases significantly along an axis predominately oriented between North West and South East.

The CV scores obtained for the 3030 series reveal a main North-West to South-East spatial gradient (Fig. 5). The lowest CV values are located along the Atlantic and northern Cantabric coast to the North-West (a minimum of 0.18 in December at Ponte de Lima, north of Porto, Portugal), while the highest values of CV are found on the Mediterranean coast (a maximum of 1.64 in November at La Pobla del Duc, Valencia). During May, the areas with the highest values of CV are spread along the southern coastland areas (Andalucía).

Similar results to the r index show the spatial distribution of CV between the observed and reconstructed precipitation. It is evident from Fig. 5 that CV mirrors the r spatial distribution. Notwithstanding differences appear at the end of winter and in the spring months.

HESSD
9, 6935–6977, 2012

The errors (residuals) are spatially heterogeneous and normally distributed around the null value (not shown), however the width of the left half of the distribution (when predictions < observations) is usually twice the width of the right half; this asymmetry of the residuals is a common feature of regression models that predict precipitation because observed extreme precipitation values at the right tail of the distribution are more difficult to reproduce (Spellman, 2000; Storch and Zwiers, 1999).

Finally, there are no significant differences between observed and predicted mean monthly rainfall totals (not shown). The worst feature of the predicted series is the substantial under-prediction of interannual variability in eastern IP, where for each month the predicted standard deviations are significantly lower (up to ten time smaller) than observed for the majority of series (not shown, but similar to Fig. 4).

3.2 Number and type of predictor WTs

The spatial distribution of the number of predictors retained (i.e. WT) for the models are shown for each month in Fig. 6. A small number of series (5 %) were modelled by one predictor only; all of them are concentrated over the Mediterranean Coast. Series with 2 predictors are more widespread (17 %), particularly in March. The most abundant series are those with 3 predictors (28 %), and they are homogeneously distributed all over IP. On the other side models requiring either 4 predictors (24 % series) and 5 predictors (15 % series) tend to be clustered in the western and central sectors of IP. Series with 6 predictors (6 %) are usually not found on the Mediterranean Coast, but are numerous in Portugal and Andalusia in south Spain. Series with 7 and 8 predictors (the 1 % and 0.2 %, respectively) are mostly confined to southern Portugal.

In general terms there is a rough longitudinal spatial gradient in the number of WTs from West (more) to the East (less) (Fig. 6). Temporally, the mean number of WTs scores its maximum in October (3.9 WTs mean value), November (3.8 WTs), December (3.6 WTs) and January (3.5 WTs), while the minimum values correspond to May (2.7 WTs), March (2.8 WTs) and April (2.9 WTs). Usually series with a high number of WTs have better correlations and lower CV scores than series with fewer predictors.

HESSD
9, 6935–6977, 2012

We present in Table 3 the monthly percentage of days that fall in each WT class (column A) and the percentage estimation of precipitation (in mm) by WTs over the total observed monthly precipitation (column B). Please note that B columns do not sum 100 because we did not present the constant term, and because the value of B columns are calculated dividing the amount (mm) of precipitation predicted by the amount (mm) of precipitation observed, and the result can be different to 100 %. The percentage of relative contribution of each WT to the observed monthly precipitation varies considerably from serie to serie and from month to month. The global monthly relative contribution of all WTs can be found in the last row of Table 3. The highest global values are found in January (79.4 %), the lowest in May (55.4 %). On average, the global relative contribute of all 26 WTs to mean monthly rainfall from October to May is about 66.7 %, and the five wettest WTs contribute to more than half (51.2 %) of total monthly precipitation, namely the Westerly (20.3 %), Pure Cyclonic (13.2 %), South-westerly (9.4 %), North-westerly (4.8 %) and Northerly (3.5 %) (see column Weather types of Table 3).

The contribution of Westerly (W) weather types rises gradually from October to March and then decrease monotonically until May when the lowest values are reached; the same pattern is observed in South-westerly (SW), while the maximum is achieved in December. On the contrary, the contribution of NW and N WTs shows high monthly oscillations from October to May. Pure cyclonic (C) type is a special case because it drops abruptly to 2.1 % in January, while during all other months it never falls below 10 % and monthly oscillations are quite low.

It is worth noting that on a monthly average, the 8 directional WTs contribute to 40.9 % of global monthly precipitation, the 9 cyclonic WTs contribute to 21.1 %, while the 9 anticyclone WTs only contribute 4.7 %. On the other hand, the maximum mean value relative contribution to total precipitation of directional WTs can be observed in winter, while for cyclonic WTs this maximum contribution is located in spring or autumn.

As a global resume, in Fig. 7 we present the spatial distribution of relative WTs contribution to monthly precipitation. The mean value of the precipitation contribution by

HESSD
9, 6935–6977, 2012

the WTs identified by model, irrespectively of their number, suggests some interesting features at spatial level. In central, western and south-western areas the mean value contribution of WTs to monthly precipitation is usually over 70 %, and sometimes even above 90 %. However, in a few restricted areas less than 50 % of monthly precipitation are reproduced by the WTs based models, particularly along the Mediterranean coast, and inland areas such as the Ebro Basin in February, April, and May. A second interesting result can be appreciated in the northern mountainous sector of Iberia; this area is very humid, but the WTs only reproduce a maximum of 70 % of monthly precipitation that could be due to a systematic effect of mountain chain parallel to the coast enhancing a local forcing.

The variation of the different WTs spatial distribution and their contribution to monthly precipitation is high. We present an example for January (Fig. 8) because this is the month in which the model prediction achieves higher proportion of total precipitation by WTs (79.4 %).

During January the selected WTs vary greatly from region to region. The W, SW and C types are the most spatially distributed of the five wettest WTs (W, SW, C, NW, N, see Table II) and they contribute to a monthly precipitation over 10 % of monthly totals. The relevance of their contribution can be seen to extend over all areas except the northern coast, were the NW and N predictors are predominate with their anticyclonic counterparts (A.NW and A.N, not shown in Fig. 8). The S type is globally weaker but strongly affects Mediterranean coastland (Fig. 8).

Pure Cyclonic (C) is the wettest of the cyclonic types (Fig. 8). It has a strong influence (>30 %) on precipitation in the North East (Ebro Valley and Catalonia) and southern coastland of Andalucía); it also contribute to a lesser extent (between 10–30 %) in extended areas of inland IP, but it does not contribute to the North West (Galicia), Northern coastland and to the South East (Fig. 8). The other cyclonic WTs contribute with a very low proportion of monthly precipitation, do not show any clear spatial pattern, or have a small influence on a limited area.

HESSD
9, 6935–6977, 2012

The majority of the anticyclonic types were rarely selected as predictor WTs; only anticyclonic A.NW and A.N types have a moderate contribution along the northern coast, while anticyclonic A.SW contributes scarcely to rainfall in Galicia and Andalusia (S Spain).

4 An example of reconstruction of long term monthly precipitation in the IP

The regression model has been applied to three very long monthly precipitation series of IP, specifically Lisbon, Madrid and Valencia, showing a strong West-East latitudinal gradient from oceanic (Lisbon), to continental (Madrid) to Mediterranean coast (Valencia) conditions. Then we would expect a good agreement at Lisbon and Madrid and to a lesser extent in Valencia accordingly the previous results of validation period (see Figs. 4 and 5). The precipitation regime at Lisbon has a maximum during the winter months. In Madrid the precipitation regime is dominated by a symmetric bimodal spring-autumn, while in Valencia, the bimodal rainfall regime exhibits a maximum during autumn.

In Table 4, we show the CV scores calculated for the independent validation period 1864–1947 and confronted with CV scores for the reference period 1948–2003. The difference between the reference CV and the CV achieved during 1864–1947 was divided by the reference CV, in order to compute the relative change in CV (as a percentage of the CV over the reference period).

Considering only the reference period 1948–2003, it is evident that the CV score really improves from east to west, ranging from 1.08 for Valencia in October, up to a minimum of 0.37 for Lisbon in December. As expected the CV scores obtained for the independent Validation period (1864–1947) are up to 75 % higher (worse) than CV scores for period 1948–2003. CVs only diminish in Valencia during October, January and April, but this is not really an improvement, because CV scores were already very high (>0.80), and the new CVs never fall below 0.70.

HESSD
9, 6935–6977, 2012

In order to compare observed and modelled values we show (Fig. 9) the predicted and observed January values during the whole period (1864–2003) at Lisbon, Madrid and Valencia stations. Lisbon station shows a good agreement even during the first period 1864–1947. Madrid station shows a good agreement during 1948–2003, however during 1864–1947 the CV scores raise up to 91 % higher. Valencia station always shows the highest value in CV, even during calibration period 1948–2003, so the model is not able to reconstruct the rainfall in this area as is capable for inland and western IP, as already discussed in Sect. 3.1. Finally, the three stations show a general overestimation of predicted precipitation during the 19th century.

5 River flow modeling

Weather Type classifications have been used for different purposes in the context of hydrological research, particularly their relation with precipitation, drought and river discharge (including floods). Hanggi et al. (2011) analysed changes in number of days at seasonal and annual scales of the Alpine Weather Types in Switzerland, and they found that changes in WTs are important to explain the observed changes in precipitation amounts. However, none of the analysed WT classes could be identified as the key factor controlling precipitation variability, moreover, the driving forces behind the observed changes in the WTs still remain unclear. In Portugal Andrade et al. (2011) studied the relationship between the prevalent weather types conditions during the extremely wet winter of 2009–2010 and some hydrological impacts. The authors provide a comparison with previous wet winters and concluded that not only Wts related to the North Atlantic Oscillation pattern explained the positive anomalies of that winter. Another set of papers related WTs with drought: Fowler and Kilsby (2002) analysed in Britain the period 1881 to 1998, and confirmed the need for the reassessment of return period estimates for contemporary drought events. Fleig et al. (2011) related severe hydrological droughts and WTs as a starting point to improve the understanding

HESSD
9, 6935–6977, 2012

of hydroclimatological processes involved in the development of regional hydrological drought in north-western Europe.

Obviously many previous works deal (with or without WTs) with relationship between precipitation and river discharge (see Wilby et al., 2011; Troy et., 2012, as a recent example). Finally, several researchers focussed on WT relationship and river discharge. Auffray et al. (2011) reconstructed the hydrometeorological scenario that has lead to the 1859 historical flood of the Isere river while Fowler et al. (2000) analysed the relationship between WT and water resources by means of precipitation series generated from WTs. Kilsby et al. (2007) presented a weather generator for analyzed climate-hydrological impact and their scenarios, and recently Pappenberger et al. (2011) analyzed the European Flood Alert System based on European Centre for Medium Range Weather Forecasts over a period of 10 yr.

The methodology developed in the present paper has been applied to the hydrological response of three of the main international rivers of IP (Duero, Tagus, and Guadiana) all of them draining from east to west. The rational for these links between is that the large river basins act as spatial and temporal integrator of climatic variables that control river flow amounts, i.e. precipitation (rain and snow), temperature, and related evapotranspiration (Trigo et al., 2004; Gámis-Fortiz et al., 2010). Model performance was evaluated using the Coefficient of Variation defined in Eq. (2) replacing monthly rainfall amount with monthly river discharge, and using the Skill Score (SS). The SS is a measure of the relative accuracy of a model with respect to a standard reference model (Murphy, 1988); it is equivalent to the percentage improvement over a reference or benchmark model (Wilks, 2005). A SS based on the Root Mean Square Error was used in this paper with the climatology ($RMSE_{CLIM}$) of the river discharge as a reference, following Eq. (3):

$$SS_{CLIM}(RMSE) = \frac{RMSE - RMSE_{CLIM}}{0 - RMSE_{CLIM}} \quad (3)$$

The SS_{CLIM} is positive if the RMSE of the model is lower than the RMSE of the reference model, and negative otherwise.

HESSD
9, 6935–6977, 2012

High resolution reconstruction of monthly precipitation

N. Cortesi et al.

As an example we show the interannual variability of both observed and modelled January river flow between 1956–2003 and relative to all three rivers considered (Fig. 10). It is immediately noticeable the relatively good capacity of these simple models to reproduce the main characteristics of the observed river flow variability, with all three rivers presenting significant correlation coefficients; Duero ($r = 0.59$), Tagus ($r = 0.69$), Guadiana ($r = 0.61$). Nevertheless, as stressed previously, one should be careful to consider the overall quality of models based on correlation coefficients alone. Thus we now focus on the overall quality of models based in terms of obtained CV scores (Table 5), showing that the Duero is the river with the lowest mean monthly CV (0.52), while Tagus and Guadiana discharges are more difficult to reproduce (mean CV = 0.93 and 1.08, respectively). Better model performance was achieved from November to March for all the three basins. In the Duero basin the monthly discharge with highest prediction is achieved during February, being the contribution of different WTs types dominated by W (48 %). In the Guadiana catchment the highest contribution of WTs is achieved in February under W (90 %), while in the Tagus catchment the maximum monthly contribution is achieved in November under W (66 %). The results show that the WTs affect differently both at spatial and temporal scales.

The SS_{CLIM} shows that the WTs improve the reference model persistence-driven for all three river discharges from September to July except December in the Duero and Tagus river, while in the Guadiana the results are more variable at monthly level (Table 6). The maximum SS_{CLIM} is +27 % for Tagus discharge, during January and February. In Duero basin the maximum improvement (+18 %) is achieved in January and March and in Guadiana basin in February (+25 %). Human control by dam management can be one of the main reasons for different basin response, namely by introducing delays between the atmospheric circulation and river flow discharges. Further analyses, in progress, at monthly level for all the different main catchment of the IP would be able to produce important results to be considered in water planning at national and supranational level.

6 Discussion and conclusions

The circulation weather type classification devised by Trigo and DaCamara (2000) has been successfully applied to reconstruct and validate monthly precipitation for the 56 yr of the period 1948–2003 at 3030 Iberian site locations by means of a leave-one-out cross-validation method applied to a non-negative least-square linear regression model. The results indicate that the use of circulation weather types in a forward regression method is a useful framework for the analysis of mean monthly rainfall on the Iberian Peninsula, with a mean monthly global CV always below 0.6 and the possibility to improve the model further eliminating the systematic errors.

The results of the regression model show agreement with previous studies (Goodess et al., 2002; Spellman, 2000; Trigo and DaCamara, 2000), although these use coarser resolution SLP data and lower density precipitation data. As expected, the most accurate predictions are achieved in western locations of IP and there is a progressive decrease in accuracy to the east, where spatial variability of rainfall is very high and cannot be captured by the model, partially because precipitation events there are not well related with synoptic scale atmospheric circulation. This means that even in non-summer seasons, modelling outcomes along the Mediterranean coast are obtained with less confidence. Unfortunately this is an area where accurate impact scenarios are of most value due to the growing mismatch between water resource supply and demand, and where human and economic activities are concentrated.

In general terms, the models achieve the best results where precipitation is more regular and more abundant (western areas), and has less accuracy on the contrary (Mediterranean coast). In this context, the temporal precipitation variability that characterizes the eastern Mediterranean fringe of IP is due to a very low number of WTs. In this regard, past (and future) changes of monthly frequency of just 1 or 2 WTs classes are bound to have a significant impact in precipitation totals. On the other hand, the precipitation variability observed in western sectors of IP appears to be related with a larger number of WTs, thus ensuring that the precipitation in this area is

HESSD
9, 6935–6977, 2012

less susceptible to changes in frequency of occurrence of just 1 or 2 classes. As a consequence, temporal changes in WTs responsible of precipitation affecting Mediterranean coast would have more dramatic effects than single changes in WTs affecting to the west.

In addition, the regression model had been applied to three very long monthly precipitation series of Iberia Peninsula, specifically Lisbon, Madrid and Valencia for the 1864–1947, showing a strong West-East latitudinal gradient from oceanic (Lisbon), to continental (Madrid) to Mediterranean coast (Valencia) conditions with Lisbon having the better CVs scores and Valencia the worst CVs scores. It was shown therefore, that the use of WTs can be of added value when reconstructing precipitation time series. We foresee the use of these models in follow-up work in order to obtain monthly precipitation fields at very high resolution (500 locations for the whole IP) since the 1850s with reasonable accuracy.

Acknowledgements. Contact Grant Sponsor Ministerio de Ciencia e Innovación Spanish Goverment), project Impactos Hidrológicos del Calentamiento Global en España (HIDROCAES) (CGL2011-27574-C02-01). Nicola Cortesi is FPI-PhD student supported by Ministerio de Cultura, (Spanish Goverment). Alexandre M. Ramos was supported through Portuguese Science Foundation (FCT) through grant BD/46000/2008. Ricardo Trigo was supported by Project DISASTER – GIS database on hydro-geomorphologic disasters in Portugal: a tool for environmental management and emergency planning (PTDC/CS-GEO/103231/2008) funded by the Portuguese Foundation for Science and Technology (FCT).

References

Andrade, C., Santos, J. A., Pinto, J. G., Corte-Real, and J.: Large-scale atmospheric dynamics of the wet winter 2009–2010 and its impact on hydrology in Portugal, Clim. Res., 46, 29–41, 2011.

Ansell, T., Jones, P. D., Allan, R. J., Lister, D., Parker, D. E., Brunet-India, M., Moberg, A., Jacobeit, J., Brohan, P., Rayner, N., Aguilar, E., Alexandersson, H., Barriendos, M., Brazdil, R., Brandsma, T., Cox, N., Drebs, A., Founda, D., Gerstengarbe, F., Hickey, K., Jonsson,

HESSD
9, 6935–6977, 2012

T., Luterbacher, J., Nordli, O., Oesterle, H., Rodwell, M., Saladie, O., Sigro, J., Slonosky, V., Srnec, L., Suarez, A., Tuomenvirta, H., Wang, X., Wanner, H., Werner, P., Wheeler, D., and Xoplaki, E.: Daily mean sea level pressure reconstructions for the European – North Atlantic region for the period 1850–2003, J. Climate, 19, 2717–2742, 2006.

Auer, I., Bohm, R., Jurkovic, A., Orlik, A., Potzmann, R., Schoner, W., Ungersbock, M., Brunetti, M., Nanni, T., Maugeri, M., Briffa, K., Jones, P., Epthymiadis, D., Mestre, O., Moisselin, J. M., Begert, M., Brazdill, R., Bochniker, O., Cegnar, T., Gajic-Capka, M., Zaninovic, K., Majstorovic, Z., Szalai, S., Szentimrey, T., and Mercalli, L.: A new instrumental precipitation dataset for greater Alpine region for the period 1800–2002, Int. J. Climatol., 25, 139–166, 2005.

Auffray, A., Clavel, A., Jourdain, S., Ben Daoud, A., Sauquet, E., Lang, M., Obled, C., Panthou, G., Gautheron, A., Gottardi, F., and Garcon, R.: Reconstructing the hydrometeorological scenario of the 1859 flood of the Isere river, Houille Blanche-Revue Internationale de l'eau, 1, 44–50, 2011.

Bárdossy, A. and Pegram, G.: Downscaling precipitation using regional climate models and circulation patterns toward hydrology, Water Resour. Res., 47, W04505, doi:10.1029/2010WR009689, 2011.

Brunetti, M., Maugeri, M., Monti, F., and Nanni, T.: Temperature and precipitation variability in Italy in the last two centuries from homogenised instrumental time series, Int. J. Climatol., 26, 345–381, 2006.

de Castro, M., Martín-Vide, J., and Alonso, S.: El clima de España: pasado, presente y escenarios de clima para el siglo XXI, in Impactos del cambio climatico en España, Ministerio Medio Ambiente, Madrid, 2005.

de Luis, M., Gonzalez-Hidalgo, J. C., Longares, L. A., and Stepanek, P.: Regímenes estacionales de la precipitacion en la vertiente mediterranea de la Península Iberica, in Cambio climatico regional y sus impactos, Asociacion Española de Climatología, Tarragona, 81–90, 2008.

de Luis, M., Gonzalez-Hidalgo, J. C., Longares, L. A., and Stepanek, P.: Seasonal precipitation trends in the Mediterranean Iberian Peninsula in second half of 20th century, Int. J. Climatol., 29, 1312–1323, 2009.

de Luis, M., Brunetti, M., Gonzalez-Hidalgo, J. C., Longares, L. A., and Martin-Vide, J.: Changes in seasonal precipitation in the Iberian Peninsula during 1946–2005, Global Planet. Change, 74, 27–33, 2010.

HESSD
9, 6935–6977, 2012

High resolution reconstruction of monthly precipitation

N. Cortesi et al.

Demuzere, M., Trigo, R. M., Vila-Guerau de Arellano, J., and van Lipzig, N. P. M.: The impact of weather and atmospheric circulation on O3 and PM10 levels at a rural mid-latitude site, Atmos. Chem. Phys., 9, 2695–2714, doi:10.5194/acp-9-2695-2009, 2009.
Efroymson, M. A.: Multiple regression analysis. Mathematical Methods for Digital Computers, edited by: Ralston, A. and Wilf, H. S., Wiley, 1960.
Fleig, A. K., Tallaksen, L. M., Hisdal, H., and Hannah, D. M.: Regional hydrological drought in north-western Europe: linking a new Regional Drought Area Index with weather types, Hydrol. Process., 25, 1163–1179, 2011.
Fowler, H. J. and Kilsby, C. G.: A weather-type approach to analysing water resource drought in the Yorkshire region from 1881 to 1998, J. Hydrol., 262, 177–192, 2002.
Fowler, H. J., Kilsby, C. G., and O'Connell, P. E.: A stochastic rainfall model for the assessment of regional water resource systems under changed climatic condition, Hydrol. Earth Syst. Sci., 4, 263–281, doi:10.5194/hess-4-263-2000, 2000.
Gámis-Fortis, S., Esteban-Parra, M. J., Trigo, R. M., and Castro-Diez, Y.: Potential predictability of an Iberian river flow based on its relationship with previous winter global SST, J. Hydrol., 385, 343–349, doi:10.1016/j.jhydrol.2010.02.010, 2010
García-Herrera, R., Hernández, H., Paredes, D., Barriopedro, D., Correoso, J. F., and Prieto, L.: A MASCOTTE-based characterization of MCSs over Spain, 2000–2002, Atmos. Res., 73, 261–282, 2005.
García-Herrera, R., Paredes, D., Trigo, R. M., Trigo, I. F., Hernández, H., Barriopedro, D., and Mendes, M. T.: The outstanding 2004–2005 drought in the Iberian Peninsula: the associated atmospheric circulation, J. Hydrometeorol., 8, 483–498, 2007.
Gonzalez-Hidalgo, J. C., Lopez-Bustins, J. A., Stepanek, P., Martín-Vide, J., and de Luis, M.: Monthly precipitation trends on the Mediterranean fringe of the Iberian Peninsula during the second half of the 20th century (1951–2000), Int. J. Climatol., 29, 1415–1429, 2009.
Gonzalez-Hidalgo, J. C., Brunetti, M., and de Luis, M.: A new tool for monthly precipitation analysis in Spain: MOPREDAS database (Monthly precipitation trends December 1945–November 2005), Int. J. Climatol., 31, 715–731, 2011.
Goodess, C. M. and Jones, P. D.: Links between circulation and changes in the characteristics of Iberian rainfall, Int. J. Climatol., 22, 1593–1615, 2002.
Goodess, C. M. and Palutikof, J. P.: Development of daily rainfall scenarios for southeast Spain using a circulation-type approach to downscaling, Int. J. Climatol., 18, 1051–1083, 1998.

HESSD
9, 6935–6977, 2012

Hanggi, P., Jetel, M., Kuttel, M., Wanner, H., and Weingartner, R.: Weather type-related trend analysis of precipitation in Switzerland, Hydrol. Wasserbewirts., 55, 140–154, 2011.
Huth, R., Beck, C., Philipp, A., Demuzere, M., Ustrnul, Z., Cahynová, M., Kyselý, J., and Tveito, O. E.: Classifications of Atmospheric Circulation Patterns, Annals of the New York of Sciences, 1146, 105–152, 2008.
Jenkinson, A. F. and Collison, F. P.: An initial climatology of gales over the North Sea, Synoptic Climatology Branch Memorandum, No. 62, Meteorological Office, Bracknell, 1977.
Jones, P. D., Hulme, M., and Briffa, K. R.: A comparison of Lamb circulation types with an objective classification scheme, Int. J. Climatol., 13, 655–663, 1993.
Kassomenos, P.: Synoptic circulation control on wild fire occurrence, Phys. Chem. Earth, 35, 544–552, 2010.
Kilsby, C. G., Jones, P. D., Burton, A., Ford, A. C., Fowler, H. J., Harpham, C., James, P., Smith, A., and Wilby, R. L.: A daily weather generator for use in climate change studies, Environ. Modell. Softw., 22, 1705–1719, 2007.
Lorenzo-Lacruz, J., Vicente-Serrano, S. M., López-Moreno, J. I., González-Hidalgo, J. C., and Morán-Tejeda, E.: The response of Iberian rivers to the North Atlantic Oscillation, Hydrol. Earth Syst. Sci., 15, 2581–2597, doi:10.5194/hess-15-2581-2011, 2011.
Kassomenos, P.: Synoptic circulation control on wild fire occurrence, Phys. Chem. Earth, 35, 544–552, 2010.
Miranda, P., Coelho, F., Tomé, A., and Valente, A.: 20th century Portuguese climate and climate scenarios, Climate Change in Portugal: Scenarios, Impacts and Adaptation Measures, SIAM, edited by: Santos, F. D., Forbes, K., and Moita, R., Gradiva, 27–83, 2002.
Mosmann, V., Castro, A., Fraile, R., Dessens, J., and Sánchez, J. L.: Detection of statistically significant trends in the summer precipitation of mainland Spain, Atmos. Res., 70, 43–53, 2004.
Murphy, A. H.: Skill scored based on the measured errors and their relationshiops to the correlation coefficient, Mon. Weather Rev., 116, 2417–2424, 1988.
Pappenberger, F., Thielen, J., and Del Medico, M.: The impact of weather forecast improvements on large scale hydrology: analysing a decade of forecasts of the European Flood Alert System, Hydrol. Process., 25, 1091–1113, 2011.
Paredes, D., Trigo, R. M., García-Herrera, R., and Trigo, I. F.: Understanding precipitation changes in Iberia in early spring: weather typing and storm-tracking approaches, J. Hydrometeorol., 7, 101–113, 2006.

HESSD
9, 6935–6977, 2012

High resolution reconstruction of monthly precipitation

N. Cortesi et al.

Philipp, A., Bartholy, J., Beck, C., Erpicum, M., Esteban, P., Fettweis, X., Huth, R., James, P., Jourdain, S., Kreienkamp, F., Krenner, T., Lykoudis, S., Michalides, S. C., Pianko-Kluczynska, K., Post, P., Rasilla-Alvarez, D., Schiemann, R., Spekat, A., and Tymvios, F. S.: Cost733cat – a database of weather and circulation type classifications, Phys. Chem. Earth, 35, 360–373, 2010.

Prudhomme, C. and Genevier, M.: Can atmospheric circulation be linked to flooding in Europe?, Hydrol. Process., 25, 1180–1190, 2011.

Ramos, A. M., Lorenzo, M. N., and Gimeno, L.: Compatibility between modes of low frequency variability and Circulation Types: a case study of the North West Iberian Peninsula, J. Geophys. Res., 115, D02113, doi:10.1029/2009JD012194, 2010.

Ramos, A. M., Ramos, R., Sousa, P., Trigo, R. M., Janeira, M., and Prior, V.: Cloud to ground lightning activity over Portugal and its association with Circulation Weather Types, Atmos. Re., 101, 84–101, 2011.

Sanchez-Arcilla, A., Mosso, C., Sierra, J. P., Mestres, M., Harzallah, A., Senouci, M., and El Raey, M.: Climatic drivers of potential hazards in Mediterranean coasts, Reg. Environ. Change, 11, 617–636, 2011.

Santos, J. A, Corte-Real, J., and Leite, S. M.: Weather regimes and their connections to the winter rainfall in Portugal, Int. J. Climatol., 25, 33–50, 2005.

Serrano, A., Garcia, J. A., Mateos, V. L., Cancillo, M. L., and Garrido, J.: Monthly modes of variation of precipitation over the Iberian peninsula, J. Climate, 12, 2894–2919, 1999.

Spellman, G.: The use of an index-based regression model for precipitation analysis on the Iberian Peninsula, Theor. Appl. Climatol., 66, 229–239, 2000.

Tomás, C., Pablo, F., and Soriano, F. L.: Circulation weather types and cloud to ground flash density over Iberian Peninsula, Int. J. Climatol., 24, 109–123, 2004.

Trigo, R. M. and DaCamara, C. C.: Circulation weather types and their impact on the precipitation regime in Portugal, Int. J. Climatol., 20, 1559–1581, 2000.

Trigo, R. M., Pozo-Vázquez, D., Osborn, T. J., Castro-Díez, Y., Gámiz-Fortis, S. R., and Esteban-Parra, M. J.: North Atlantic Oscillation influence on precipitation, river flow and water resources in the Iberian Peninsula, Int. J. Climatol., 24, 925–944, 2004.

Troy, T. J., Sheffield, J., and Wood, E. F.: The role of winter precipitation and temperature on northern Eurasian streamflow trends, J. Geophys. Res.-Atmos., 117, D05131, doi:10.1029/2011JD016208, 2012.

HESSD
9, 6935–6977, 2012

High resolution reconstruction of monthly precipitation

N. Cortesi et al.

Valero, F., Martìn, M. L., Sotillo, M. G., Morata, A., and Luna, M. Y.: Characterization of the autumn Iberian precipitation from long term datasets: comparison between observed and hindcasted data, Int. J. Climatol., 29, 527–541, 2009.

Vicente-Serrano, S. M., Trigo, R. M., Liberato, M. L. R., López-Morenom, J.,I., Lorenzo-Lacruz, J., Beguería, S., Morán-Tejeda, H., and El Kenawy, A.: Extreme winter precipitation in the Iberian Peninsula, 2010: anomalies, driving mechanisms and future projections, Clim. Res., 46, 51–65, 2011.

von Storch, H. and Zwiers, F. W.: Statistical analysis in climate research, Cambridge University Press, UK, 1999.

Wilby, R. L.: The influence of variable weather patterns on river water quantity and quality regimes, Int. J. Climatol., 13, 447–459, 1993.

Wilby, R. L.: Modelling low-frequency rainfall events using airflow indices, weather patterns and frontal frequencies, J. Hydrol., 213, 380–392, 1998.

Wilby, R. L., Fenn, C. R., Wood, P. J., Timlett, R., and LeQuesne, T.: Smart licensing and environmental flows: Modeling framework and sensitivity testing, Water Resour. Res., 47, W12524, doi:10.1029/2011WR011194, 2011.

Wilks, D. S.: Statistical Methods in the Atmospheric Sciences: An Introduction, International Geophysics, Series 59, Academic Press, St. Louis, Missouri, USA, 2005.

HESSD
9, 6935–6977, 2012

High resolution reconstruction of monthly precipitation

N. Cortesi et al.

Table 1. The 26 classes of WTs with eight directional types, 16 hybrid types (cyclonic and anticyclonic) and two types controlled by geostrophic vorticity (A and C).

Directional types	Anticyclonic types	Cyclonic types
NE	ANE	CNE
E	AE	CE
SE	ASE	CSE
S	AS	CSE
SW	ASW	CSW
W	AW	CW
NW	ANW	CNW
N	AN	CN
	A	C

HESSD

9, 6935–6977, 2012

High resolution reconstruction of monthly precipitation

N. Cortesi et al.

Table 2. Main characteristics of the three river basins considered. Average and standard deviation values correspond to annual river flow and were obtained using the full available period. Storage volumes for Portugal and Spain were obtained for the period 1956–2003 used in this study.

River (gauging station)	Total basin area ($1000\,km^2$)	Basin area upstream gauging station ($1000\,km^2$)	Period	Average $1000 \times hm^3$	Std. dev. $1000 \times hm^3$
Douro (Pocinho)	98.4	83.0	1956–2003	13.82	5.23
Tejo (Fratel)	80.1	59.0	1956–2003	9.29	5.51
Guadiana (Pulo do Lobo)	66.9	60.9	1956–2003	3.86	3.56

HESSD
9, 6935–6977, 2012

Table 3. Percentage of estimated relative contribute to total monthly precipitation due to each of the 26 weather types.

WT	Weather Type (full name)	Oct	Nov	Dec	Jan	Feb	Mar	Apr	May	Mean
NE	Directional Northesterly	1.1	1.2	0.4	0.0	0.6	1.4	1.1	0.6	0.8
E	Directional Esterly	1.7	0.2	0.0	0.5	0.6	1.0	0.2	0.7	0.6
SE	Directional Southesterly	0.4	1.3	0.3	1.0	0.3	0.2	0.2	0.0	0.5
S	Directional South	0.0	0.2	0.1	1.2	5.1	0.2	0.2	0.1	0.9
SW	Directional Southwesterly	7.2	7.5	16.3	15.0	13.4	7.6	4.6	3.7	9.4
W	Directional Westerly	17.1	18.2	20.3	26.7	26.9	29.0	12.8	11.7	20.3
NW	Directional Northwesterly	1.2	11.3	5.9	8.2	1.8	1.0	3.9	5.2	4.8
N	Directional Northerly	3.5	1.6	1.4	3.6	2.7	6.6	1.7	7.1	3.5
	Sum of directional WTs	32.2	41.5	44.7	56.2	51.4	47.0	24.7	29.1	40.9
C	Pure Cyclonic	10.0	11.6	10.3	17.3	2.1	13.8	22.7	17.6	13.2
C.NE	Cyclonic Northesterly	0.8	2.5	2.4	0.4	0.5	0.5	0.5	0.3	1.0
C.E	Cyclonic Esterly	3.4	0.5	1.0	0.1	0.5	0.8	0.1	0.8	0.9
C.SE	Cyclonic Southesterly	3.4	5.6	2.4	1.0	3.8	1.4	0.8	0.2	2.3
C.S	Cyclonic South	6.2	1.8	0.5	1.0	0.8	0.4	0.0	0.5	1.4
C.SW	Cyclonic Southwesterly	1.2	0.1	1.3	0.0	1.4	0.0	1.1	1.3	0.8
C.W	Cyclonic Westerly	0.5	0.2	0.4	0.0	2.2	0.2	0.0	0.3	0.5
C.NW	Cyclonic Northwesterly	0.2	0.0	0.0	0.0	0.0	0.3	0.0	0.0	0.1
C.N	Cyclonic Northerly	1.7	0.2	1.6	0.0	0.1	1.1	4.0	2.8	1.4
	Sum of cyclonic types	27.4	22.5	19.9	19.8	11.4	18.5	29.2	23.8	21.6
A	Pure Anticyclonic	0.8	2.5	2.4	0.4	0.5	0.5	0.5	0.3	1.0
A.NE	Anticyclonic Northesterly	0.9	0.1	0.0	0.0	0.1	0.0	0.1	1.5	0.3
A.E	Anticyclonic Esterly	0.1	0.0	0.0	0.0	0.0	0.0	0.3	0.2	0.1
A.SE	Anticyclonic Southesterly	0.1	0.1	0.2	0.0	0.0	0.0	0.5	0.1	0.1
A.S	Anticyclonic South	0.0	0.0	0.1	0.0	0.3	0.0	0.0	0.4	0.1
A.SW	Anticyclonic Southwesterly	0.0	0.1	0.2	0.9	0.5	0.1	0.0	0.0	0.2
A.W	Anticyclonic Westerly	0.5	0.9	0.5	0.4	0.3	2.5	1.9	0.1	0.9
A.NW	Anticyclonic Northwesterly	2.0	1.0	2.0	2.0	1.0	0.0	1.0	0.0	1.1
A.N	Anticyclonic Northerly	0.0	1.0	1.0	0.0	0.0	0.0	1.0	0.0	0.4
	Sum of antycyclonic cypes	4.4	5.7	6.4	3.7	2.7	3.1	5.3	2.6	4.2
	Sum of all Weather Types	64.8	71.1	69	79.4	65.1	68.2	60.1	55.4	66.7

HESSD
9, 6935–6977, 2012

Table 4. Coefficient of variation for Lisbon, Madrid and Valencia stations (see Fig. 1) measured for two different validation periods: 1948–2003 (same as calibration period) and 1864–1947. The percentage difference between the two validation periods appears in the third line of each station.

Lisbon	Oct	Nov	Dec	Jan	Feb	Mar	Apr	May
1948–2003	0.57	0.47	0.37	0.38	0.47	0.45	0.47	0.57
1864–1947	0.60	0.59	0.49	0.48	0.51	0.57	0.64	0.80
Δ in %	5 %	23 %	31 %	28 %	8 %	26 %	36 %	40 %
Madrid	Oct	Nov	Dec	Jan	Feb	Mar	Apr	May
1948–2003	0.56	0.56	0.50	0.54	0.49	0.45	0.51	0.52
1864–1947	0.69	0.58	0.56	0.76	0.62	0.86	0.72	0.53
Δ in %	23 %	4 %	13 %	40 %	26 %	91 %	40 %	1 %
Valencia	Oct	Nov	Dec	Jan	Feb	Mar	Apr	May
1948–2003	1.08	1.02	0.75	0.97	0.99	0.85	0.81	0.78
1864–1947	0.74	1.78	0.88	0.95	1.24	1.17	0.80	0.95
Δ in %	−31 %	75 %	18 %	−2 %	25 %	37 %	−1 %	22 %

HESSD
9, 6935–6977, 2012

Table 5. Coefficient of variation for Duero, Tagus and Guadiana (see Fig. 1) monthly river discharge from 1956 to 2003.

River	Jan	Feb	Mar	Apr	May	Jun	Jul	Aug	Sep	Oct	Nov	Dec	Mean
Duero	0.68	0.75	0.58	0.55	0.39	0.34	0.45	0.42	0.36	0.30	0.62	0.76	0.52
Tagus	0.77	0.71	0.74	1.02	0.82	1.07	1.08	0.92	1.16	0.96	0.89	1.03	0.93
Guadiana	1.14	1.00	1.25	1.51	0.91	0.98	0.95	0.78	0.74	1.10	1.38	1.26	1.08

HESSD
9, 6935–6977, 2012

HESSD
9, 6935–6977, 2012

High resolution reconstruction of monthly precipitation

N. Cortesi et al.

Table 6. Skill Score SS_{CLIM} (RMSE) for Duero, Tagus and Guadiana (see Fig. 1) monthly river discharge from 1956 to 2003.

River	Jan	Feb	Mar	Apr	May	Jun	Jul	Aug	Sep	Oct	Nov	Dec	Mean
Duero	18	12	18	−2	6	13	0	−2	−1	7	5	−3	6.0
Tagus	27	27	24	−6	2	−5	−6	−7	−2	10	19	7	7.6
Guadiana	20	25	10	−4	5	2	−1	−2	8	−1	10	17	7.4

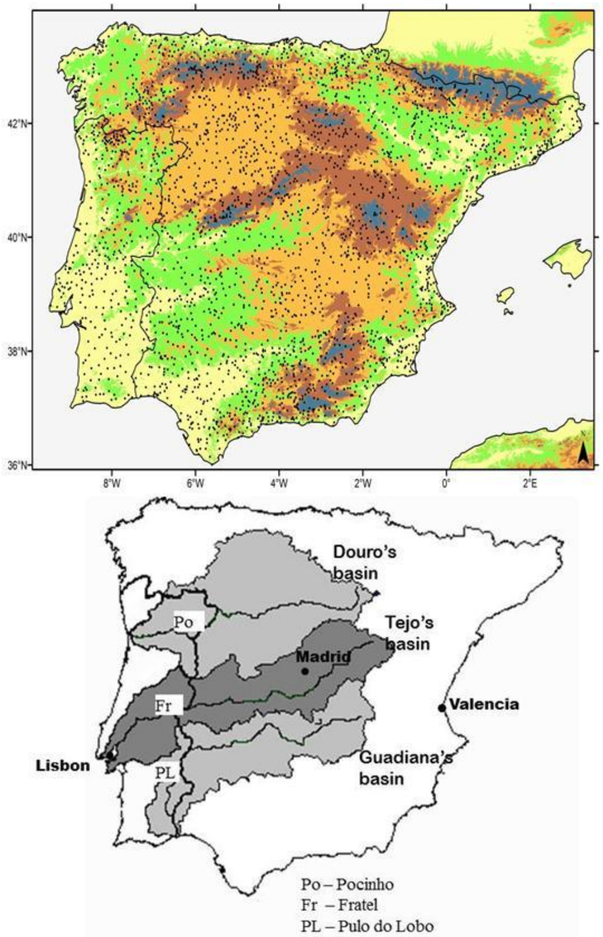

Fig. 1. Location of the 3030 monthly Iberian rainfall series.

HESSD
9, 6935–6977, 2012

Title Page
Abstract | Introduction
Conclusions | References
Tables | Figures
◀| |▶
◀ ▶
Back | Close
Full Screen / Esc
Printer-friendly Version
Interactive Discussion

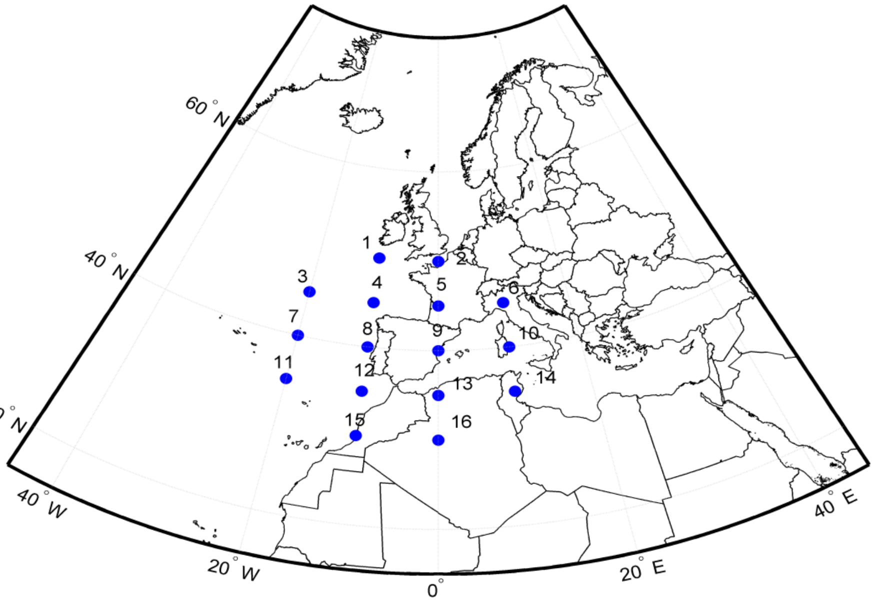

Fig. 2. Location of the 16 grid points used to compute the vorticity and flow indices.

HESSD
9, 6935–6977, 2012

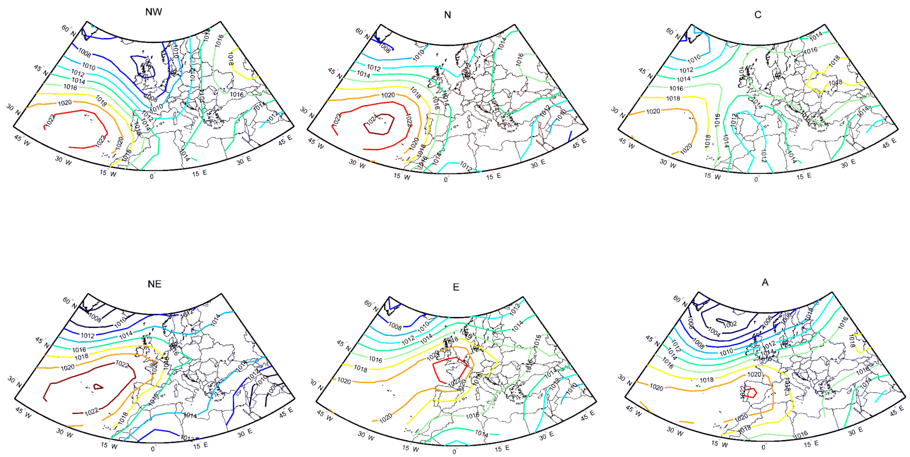

Fig. 3a. Composite map of the SLP fields for the eight directional weather types (NW, N, NE, E, SE, S, SW, W) and two vorticity weather types (C and A). Hybrid types are not shown.

HESSD
9, 6935–6977, 2012

High resolution reconstruction of monthly precipitation

N. Cortesi et al.

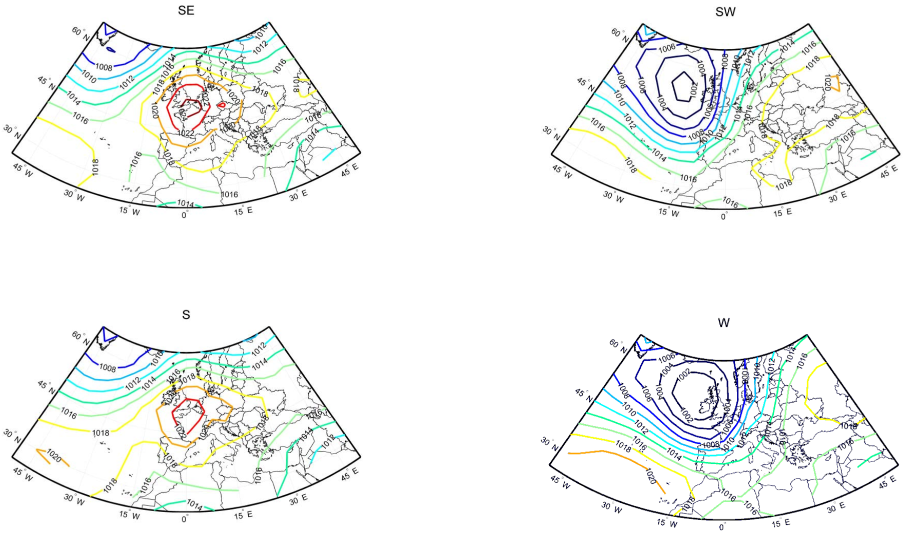

Fig. 3b. Continued.

HESSD
9, 6935–6977, 2012

High resolution reconstruction of monthly precipitation

N. Cortesi et al.

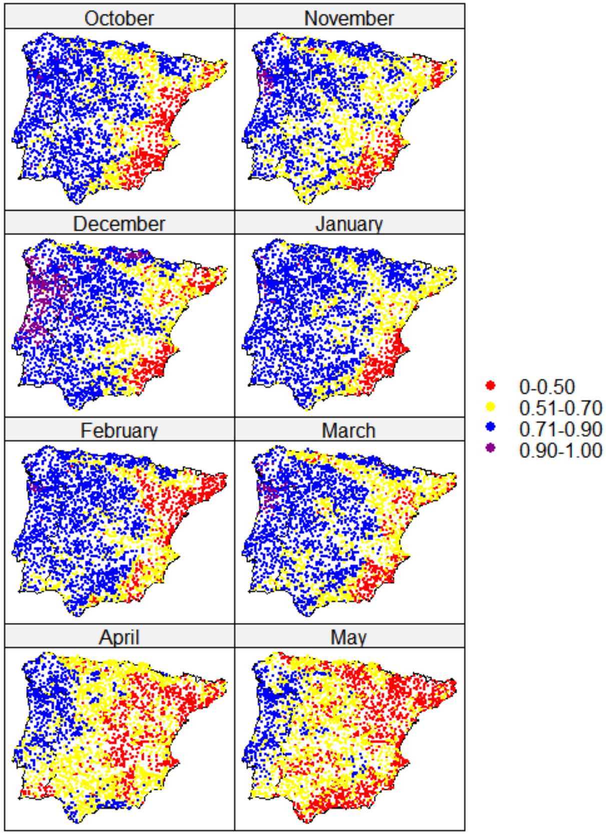

Fig. 4. Pearson correlation coefficient between predicted and observed precipitation for each month from October to May.

HESSD
9, 6935–6977, 2012

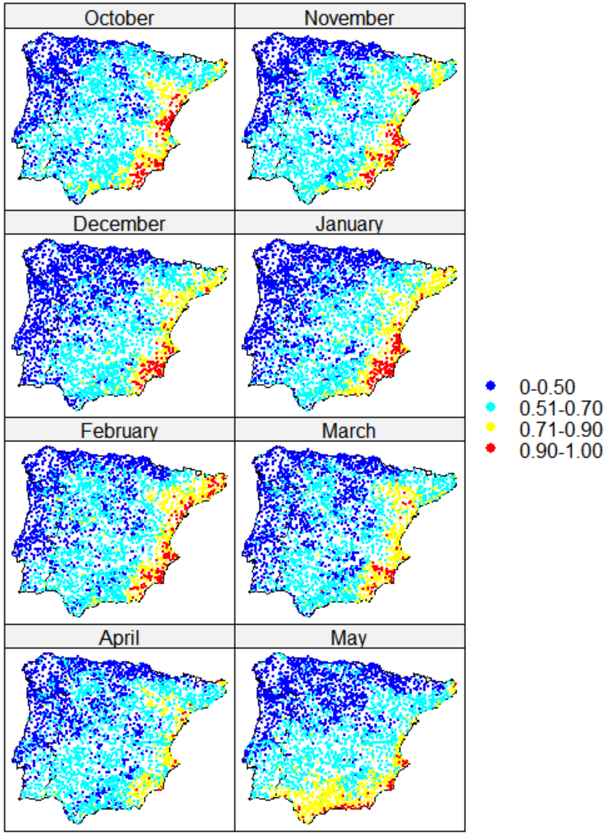

Fig. 5. Coefficient of Variation of predicted precipitation for each month from October to May. Lower CV represent better agreement between reconstruction and observations

HESSD
9, 6935–6977, 2012

High resolution reconstruction of monthly precipitation

N. Cortesi et al.

Title Page
Abstract | Introduction
Conclusions | References
Tables | Figures
◀| |▶
◀ ▶
Back | Close
Full Screen / Esc
Printer-friendly Version
Interactive Discussion

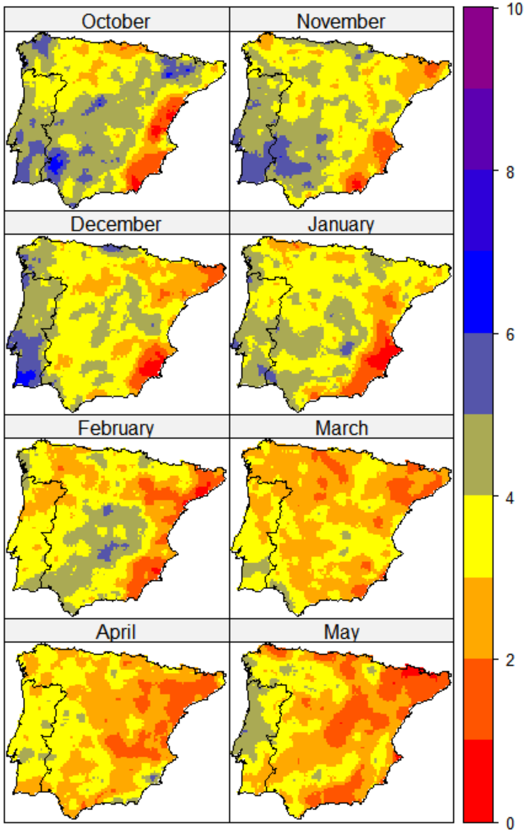

Fig. 6. Spatial and temporal distribution of the number of predictor WTs of the regression model for each month from October to May.

HESSD
9, 6935–6977, 2012

High resolution reconstruction of monthly precipitation

N. Cortesi et al.

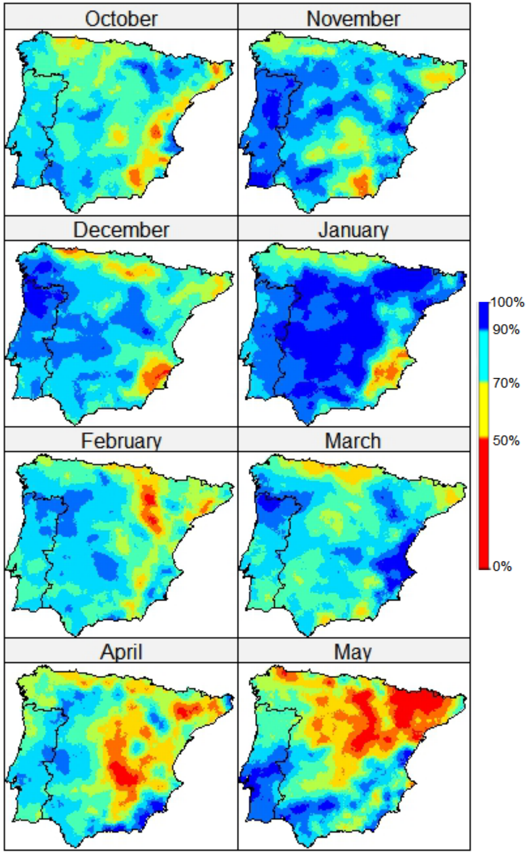

Fig. 7. Spatial distribution of the relative contribution of all WTs to monthly precipitation.

HESSD
9, 6935–6977, 2012

High resolution reconstruction of monthly precipitation

N. Cortesi et al.

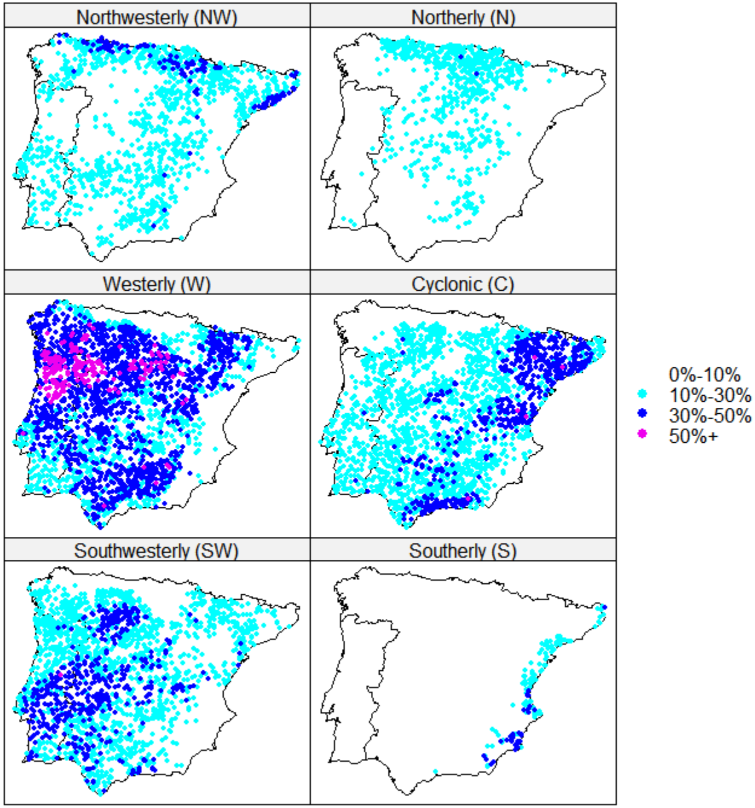

Fig. 8. Spatial distribution of the relative contribution to total January precipitation for NW, N, W, C, SW and S WTs.

HESSD
9, 6935–6977, 2012

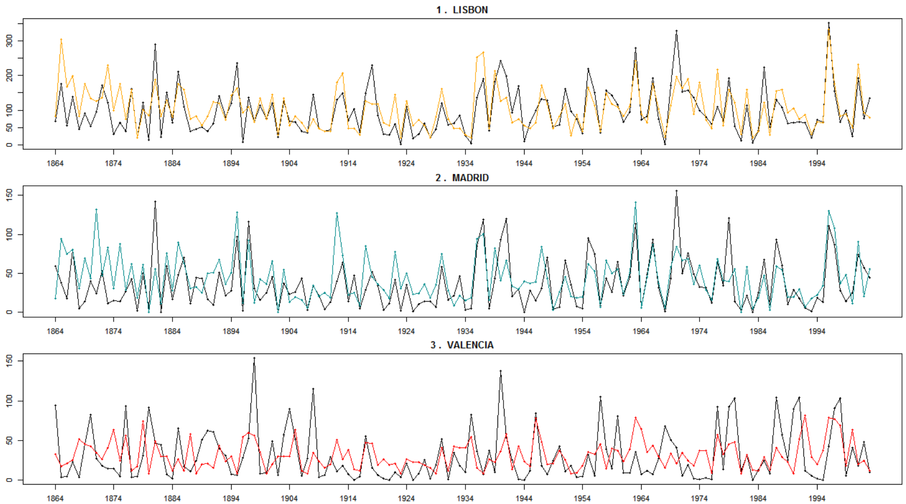

Fig. 9. January observed monthly precipitation (black line) and predicted precipitation (colored line) for the three long term stations of Valencia, Madrid and Lisbon.

HESSD

9, 6935–6977, 2012

High resolution reconstruction of monthly precipitation

N. Cortesi et al.

HESSD
9, 6935–6977, 2012

High resolution reconstruction of monthly precipitation

N. Cortesi et al.

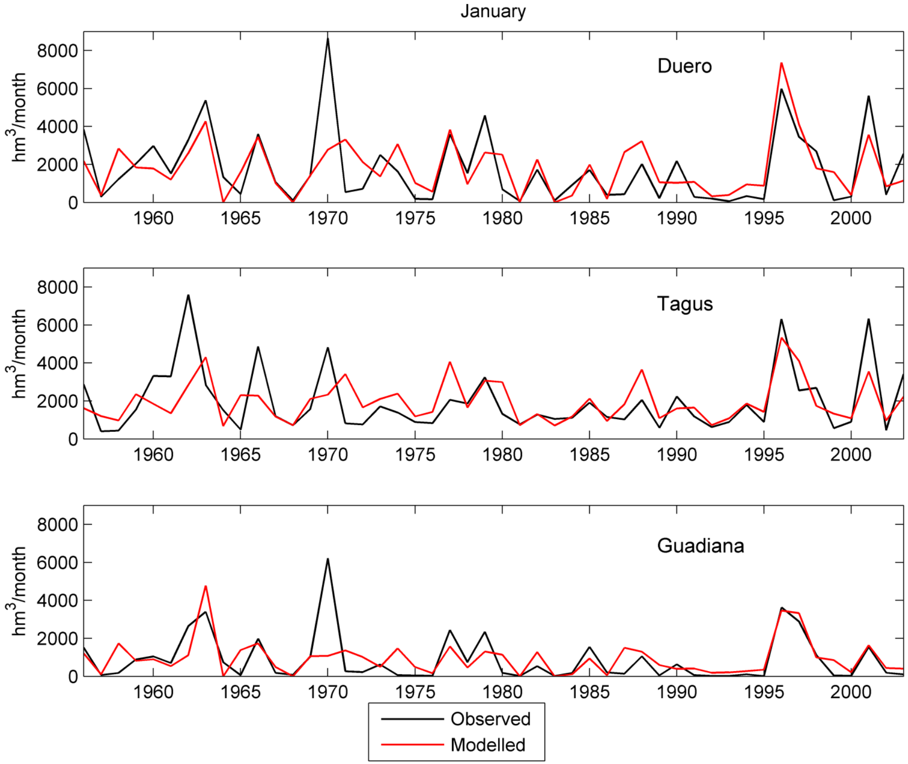

Fig. 10. January observed (black line) and predicted (red line) river flow for the Iberian rivers Duero, Tagus, and Guadiana.